

# MODELLING WAVE PROPAGATION OVER LONG DISTANCES UNDERWATER WITH PSEUDOSPECTRAL TECHNIQUES

P. Reynolds	Weidinger Associates Inc, Mountain View, California, USA
J.F.Saillant	University of Paisley, Paisley, Scotland, UK
S.Cochran	University of Paisley, Paisley, Scotland, UK

## 1 ABSTRACT

There is increasing emphasis on the use of numerical modelling techniques in almost all areas of scientific research and development, with the aim of increasing knowledge and reducing experimental and equipment costs. Naval SONAR and biomedical ultrasound device manufacturers have been intensive users of Finite Element (FE) simulation techniques since the early 1990s, and modelling is in part responsible for the extremely high quality imaging systems available today. While FE methods are well suited to the compact nature of ultrasound devices, they lose efficiency when propagation distances extend beyond tens of wavelengths. To use such discretised methods over long distances, higher order elements are required to ensure accuracy, but at increased computational cost. This paper details a pseudospectral technique, based on the use of Fourier Transforms in the spatial domain, to calculate accurately the propagation of sound over hundreds or thousands of wavelengths, requiring only two elements per wavelength, corresponding to the Nyquist limit, for satisfactory accuracy. This technique maintains many of the advantages of time domain FE, such as broadband wave propagation and frequency dependent attenuation, and is highly efficient in the parallel operation common in modern computers. Advantages and disadvantages of the technique, compared to FE, are discussed, along with examples of its use in an underwater environment, including interaction with the sea floor, with the commercially available package SpectralFlex.

## 2 INTRODUCTION

Numerical simulation methods have been a staple of the ultrasound industry for decades, with the first heavily used models derived by Mason<sup>1,2</sup>, using equivalent circuit parameters to simplify the system. These models proved accurate for predominantly one-dimensional wave propagation and remained useful despite their inclusion of non-physical components such as negative capacitors. In 1970, Krimholtz, Leedom and Matthae<sup>3</sup> updated this approach with what became known as the KLM model, the most heavily used model in the biomedical industry in the late 1970s and 1980s, with applications also in underwater SONAR. These modelling approaches proved adequate until the late 1980s when the complex structures of piezocomposite materials and arrays fully emerged.

Consideration of the use of 2D and full 3D modelling then began, through the use of Finite Element Analysis (FEA). In FEA, the system as a whole is broken down into many small component parts (finite elements), each with its own governing equations. Figure 1 shows two example FEA grids. Analysis of the interdependent elements is an ideal task for computers, and this approach had already been widely used in aerospace and civil engineering since the 1950s. While the use of FEA had been considered with piezoelectrics since the 1970s<sup>4,5</sup>, the combination of accessible computing power, industry need, and availability of FEA in a suitable form did not occur until around 1987 when Ostergaard and Pollak added the capability to the ANSYS package<sup>6</sup> and Lerch and Kaarmann demonstrated its use<sup>7</sup>.

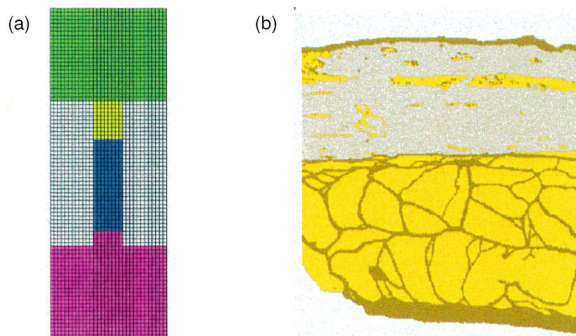


**Figure 1: Two FEA Grids. (a) a single piezoelectric element of an ultrasound array (b) a layer of skin for biomedical imaging.**

Early packages worked in the frequency domain predominantly. While useful for calculation of device characteristics such as electrical impedance spectra, this limited adoption in a technical discipline used to seeing time domain responses such as SONAR waveforms. In 1992, piezoelectric capabilities were added to PZFlex<sup>8</sup>, a time domain wave propagation code used in the defence industries for blast and impact calculations and this rapidly became the dominant FEA code in the medical ultrasound imaging community in the USA and Japan, as well as in naval SONAR.

FEA excelled at calculation of wave propagation in compact models measuring a few wavelengths in each direction, ideal for ultrasound transducers used in medical imaging and SONAR. Over the next decade, computing power increased at a sufficient rate to allow expanding needs and model sizes to be readily accommodated, but by the late 1990s it was clear that the need to simulate the propagation of waves out into the field was not being fully met. Simplified assumptions as to propagating media homogeneity, linearity, and loss were valid in fewer and fewer cases, and a new approach to solving these large problems needed to be found, particularly for SONAR.

### 3 LONG DISTANCE WAVE PROPAGATION SIMULATION

Propagation over 100s - 10,000s of wavelengths has proved generally problematic for discrete numerical methods as the scale of the model usually exceeds accessible computing power. Alternative methods such as one-dimensional approximations and ray tracing have been used with success but as the propagating medium becomes more complex and assumptions of linearity, low loss and homogeneity become less valid, the FEA type approach becomes more attractive.

All discrete numerical methods for wave propagation suffer a similar problem: for accurate results, there must be a sufficient number of elements within each wavelength to represent the stress gradients. Figure 2(a) illustrates how simple linear elements can represent a wave when 2, 4, 8 and 16 elements per wavelength are used. As can be seen, the sine wave only becomes clearly apparent at 16 elements per wavelength, and this is often suggested as a lower limit for accurate simulations. As the 'order' or complexity of an element increases, simple linear assumptions are replaced by a more complex algorithm and for smoothly varying signals such as sine waves fewer elements per wavelength are needed for accuracy. However, this reduction comes with a higher 'computational cost' per element and a reduced capacity to handle sudden discontinuities such as a water-target or water-seabed interface. Due to the need of the SONAR community to deal with models with many boundaries and significant variations in material properties, almost all available FEA packages use low order elements, either 2<sup>nd</sup> or at most 4<sup>th</sup> order.

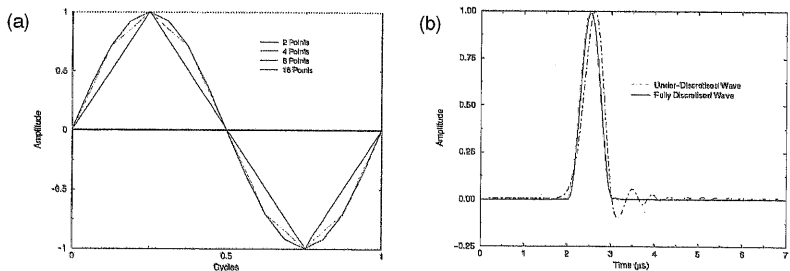
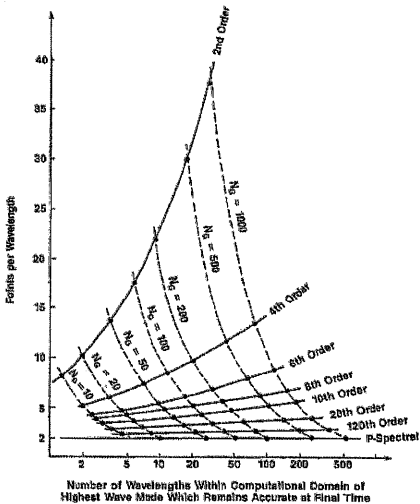


Figure 2: (a) a sine wave represented by 2, 4, 8 and 16 points with assumption of linearity, (b) pulse propagating long distance in FEA (dashed line) and analytical model (solid line).

Even at recommended element sizes, a small error per wavelength of propagation accumulates, resulting in significant error over a long propagation path. Figure 2(b) shows a half-cycle sine pulse propagated over 300 wavelengths with a 2<sup>nd</sup> order method with 20 elements/wavelength compared with the exact solution. Energy has clearly become 'dispersed' over time as different frequencies propagate at different velocities, generating an inaccurate result. The error can be reduced by increasing the mesh density beyond the recommended minimum. Figure 4 shows the minimum mesh density needed for accuracy vs distance propagated for a variety of solution 'orders'. As can be seen, at the extremely long distances needed for simulation of medical imaging or naval SONAR fields, the low order methods must significantly increase their mesh densities. Given that this is in each direction in a 2D or 3D model, it can be seen that the number of elements required for solving a large problem with low order elements becomes impossible. Use of a substantially higher order method is needed.

Figure 4: Minimum discretisation to ensure accuracy for solution methods of various order (from Fornberg<sup>10</sup>).



## 4 PSEUDOSPECTRAL METHODS

At the extreme end of Figure 4 can be seen a line labeled 'P-spectral' for 'Pseudospectral', indicating that, for this method, only the Nyquist limit of 2 elements/wavelength is needed for accurate wave propagation over any distance. This is sufficiently attractive that the oil industry has begun using it in models of geological surveys<sup>12</sup> and a natural extension is its use in SONAR applications.

Pseudospectral methods<sup>9</sup> break a structure into discrete components in a uniform grid, similar to FEA. However pressure wave propagation is solved through the use of Fourier transforms to evaluate spatial derivatives rather than element by element. This reduces the partial differential equation descriptions of acoustic wave propagation to ordinary differential equations, which can be propagated forward in time with a variety of time integration techniques. It has been shown<sup>9</sup> that the pseudospectral method is equivalent to an FE method of order  $N$ , where  $N$  is the number of elements in a given axis of the model. This leads to excellent numerical accuracy as a model typically has 100s of elements or more in each axis. Time integrator choice is typically directed towards a higher order solver such as 4<sup>th</sup> order Runge-Kutta or Adams-Bashforth to ensure accuracy not only over long simulation distances but also over long simulation times. For the implementation used in this paper, a 4<sup>th</sup> order Adams-Bashforth time integrator was chosen.

As Fourier transforms are the main computational method, the pseudospectral technique lends itself well to parallelization, and tests on shared memory systems have shown more than 90% efficiency in both 2 and 4 way simulations. This bodes well for expansion to larger computing systems, and for the future as multiple cores per processor become common.

On the other hand, pseudospectral techniques have two significant drawbacks. First, unlike most FE methods, the grid must be Cartesian and uniform, making exact placement of arbitrary boundaries difficult and introducing a potential error in location of up to half an element in scale. In many cases the discretisation of the model is finer than the most basic level, and the location error becomes manageable when compared to uncertainties in material properties. Second, the Fourier transform method is inherently periodic so that what occurs at one edge of an overall model 'loops back' and also occurs at the opposite edge, as illustrated in Figure 5.

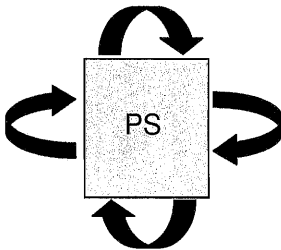


**Figure 5: 'Looping' Effect for Signals in Pseudospectral Models**

This effect is not acceptable in any practical model. However, it is easily overcome through the use of Perfectly Matched Layers (PMLs). PMLs were first suggested by Berenger<sup>10</sup> to absorb waves propagating in electromagnetic simulations, and have since been adapted to a number of other numerical simulation applications. A PML consists of elements in the numerical grid of varying attenuation designed to cause rapid decay of a wave while minimizing reflections. Typically 10 - 20 PML elements at each edge of a model can reduce signal strength by 80 - 100 dB, below noise in the system. This effect is further enhanced by the 'double-pass' effect as any 'looped' wave must propagate through the PML on both edges.

5 RESULTS

For the results presented here, the pseudospectral method for pressure wave propagation was implemented in the commercially available simulation package SpectralFlex (Weidlinger Associates Inc, Mountain View, CA, USA). Procedure, validation and verification data for this package can be found in papers by Wojcik et al<sup>11</sup>. Here, its use is illustrated through simulation of long distance, low frequency wave propagation for target discrimination in a heterogeneous environment.

The basic model comprises a 3D volume 80 wavelengths in depth, 50 wide and 30 from back to front as illustrated in Figure 6(a). The model has four layers in depth, air at the top, water, then the seabed with two layers. The archetypal signal excitation is a single-cycle sinusoid of frequency  $f = 10\text{ kHz}$  input as pressure at the upper surface of the water. This equates to a wavelength,  $\lambda \approx 15\text{ cm}$ . The target is represented by a spherical object with diameter  $d = 3\lambda$ , buried in the seabed. Spatial discretisation is set at two elements/wavelength and the material properties are as given in Figure 6(b).

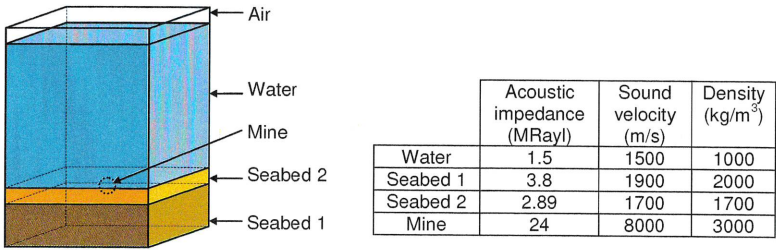


Figure 6: (a) basic model definition and (b) material properties.

To illustrate the capabilities of the pseudospectral method, results are presented from three different models, the basic model that has already been described, a similar model but with the seabed sloped at an angle  $\theta = 15^\circ$ , and a third model with a flat seabed but with an additional mine. Each simulation took 78 minutes and 216MB on a 2.8GHz Intel Desktop PC.

5.1 Basic Model

The results of the basic model are shown in Figure 7 in two forms. The upper series of results comprises 'snapshots' of wave propagation including the full SpectralFlex screen display, and the lower result shows the pressure at the surface of the water as an amplitude function in the time domain.

The first two snapshots, at  $t = 1.2\text{ ms}$  and  $t = 4.8\text{ ms}$ , show a single cylindrical wavefront propagating downwards through the water as expected. It should be noted that the colour scale for amplitude is automatically changed to maximise the clarity of presentation for each individual 'snapshot'. By the time of the third snapshot, at  $t = 6\text{ ms}$ , the single wavefront has propagated into the seabed and, because of the two layers of the seabed, has separated into four main wavefronts, two propagating downwards through the seabed, two reflected upwards from the seabed, and the fifth one almost an entire circle propagating outwards in all directions from the location of the mine. In the fourth 'snapshot', at  $t = 8.4\text{ ms}$ , the downward propagating wavefronts have disappeared, confirming that the PML approach to prevent looping effects has been successful. Three upward propagating wavefronts are still visible, the two with the largest amplitude from the water-seabed interface and the interface within the seabed. However, a wavefront from the mine is also clearly visible in this presentation.

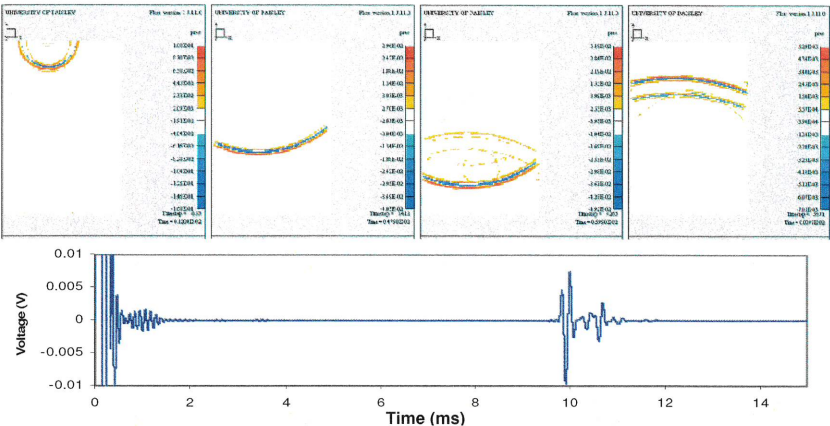


Figure 7: Basic model (top) wave propagation 'snapshots', (bottom) received signal.

The time domain result below the 'snapshots' clearly show the excitation signal and some ringing after it. There is then a very small signal between  $t = 3$  ms and  $t = 4$  ms which is attributed to imperfect operation of the PML boundary. However, the next significant received signal occurs just before  $t = 10$  ms, when the reflection from the water-seabed interface is detected. For the particular observation point selected, this is followed by a distorted second pulse comprising signals from both the lower seabed layer and the mine, the latter indicated by the very small ripple before  $t = 12$  ms. Of course, if multiple received signals were presented, the distinct wavefront from the mine would then become visible, indicating successful target detection.

5.2 Model with Sloping Seabed

The next model to be considered was one with a sloping seabed. This is illustrated in Figure 8. Here, the model is indicated schematically in the top left corner, four 'snapshots' follow it to the right, and the time domain received signal is shown below.

The first two 'snapshots' show downward wave propagation as before, and the time domain received signal also corresponds to the signal in Figure 7 for the basic model. The third 'snapshot' is, however, quite different. It is certainly still possible to see the five wavefronts shown in the basic model. Furthermore, the expected effect of the sloping seabed is clearly visible in the asymmetry of the upwardly propagating wavefronts: the notional centreline of the curve of the wavefront has shifted significantly to the right, whereas in the basic model this centreline was the same for both the downward propagating directly excited wavefronts and the upwardly propagating reflected wavefronts, approximately one third of the wave across the model from the left, corresponding to the horizontal position of the applied pressure on the surface of the water.

The difference in the third snapshot in the present case is the presence of many other lower amplitude wavefronts behind the primary ones. The reason for this is that, with a seabed slope with angle  $\theta = 15^\circ$ , spatial sampling with only two elements/wavelength results in a relatively significant stepping effect in the seabed, generating a low-amplitude wavefront from each step. This evidently obscures the signal from the mine, to the extent that it cannot be seen at all in the fourth 'snapshot'. There are three possible solutions to this problem, to be explored in further work. One is to utilise the type of 'anti-aliasing' also used to reduce stepping effects in visual displays. In the present case, this would involve smoothing by including a thin layer of intermediate material between the water



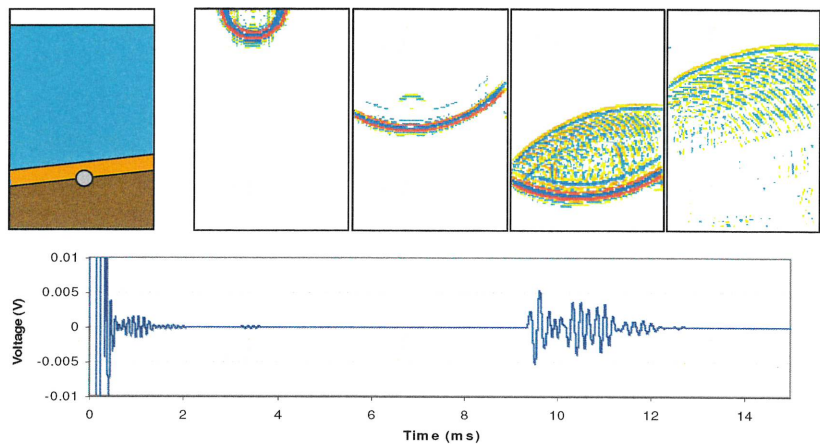


Figure 8: model with sloping seabed

and the seabed in appropriate locations relative to the steps in the seabed itself. Another solution is to vary the specific positions of the steps in the 30 front-to-back element planes so that the steps are effectively asynchronous with the wavefront. Conceptually the simplest technique is to reduce the size of the elements in the model; in the present work, this was impossible because of limitations on the computing power available. In practice, of course, a combination of all these techniques would have the maximum effect.

5.3 Model with Two Mines

The final model considered here is the same as the basic model, but in this case with two mines, the extra one placed to the right of the one in the centre in a cross-sectional view as illustrated in

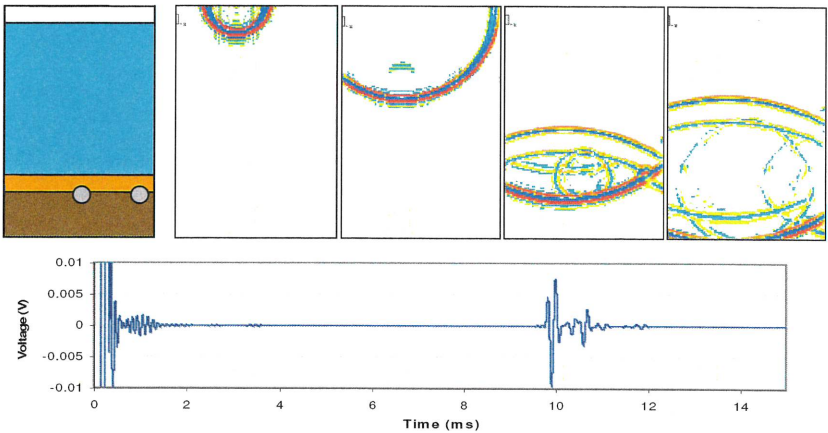


Figure 10: model with two mines

Figure 10. The first two 'snapshots' are similar to those of the basic model. However, in the third 'snapshot', an initial indication of the extra mine is visible and the fourth 'snapshot' clearly shows two circular wavefronts, one corresponding to each of the mines. The time domain received signal corresponds closely with the signal generated by the basic model but, from a close comparison, it is evident that there is a larger signal at around  $t = 12$  ms, corresponding to the reflection from the second mine, which is farther from the origin of the acoustic excitation and the point at which reception is recorded, therefore further separated from the signals from the seabed.

## 6 CONCLUSIONS

This paper has outlined the development of the finite element (FE) method for simulation of acoustic systems and highlighted a key limitation in terms of the possible size of the models that can be solved. An alternative has been presented in the form of the pseudospectral method. This is also based on a model comprising a mesh of elements, but these elements can be larger and avoid the problem of numerical inaccuracy.

Three specific models have been considered, combining heterogeneous media with simplified structures representing SONAR target detections scenarios. These have well illustrated both the valuable capabilities of the pseudospectral method and the type of limitations that may be encountered with it because of its minimal spatial sampling. Some ways to overcome the limitations have been suggested and these will be the subject of further work by the authors, along with development of the commercial SpectralFlex package including integration with FE models to allow higher spatial sampling of specific regions.

## 7 REFERENCES

1. W.P. Mason, *Electromechanical Transducers and Wave Filters*, Van Nostrand, Princeton, NJ (1948)
2. W.P. Mason, *Physical Acoustics and the Properties of Solids*, Van Nostrand, Princeton, NJ (1958)
3. R. Krimholtz, D.A. Leedom, G.L. Matthaei, "New Equivalent Circuit for Elementary Piezoelectric Transducers", *Electron. Lett.*, Vol. 6, pp. 398 - 399 (1970)
4. H. Allick and T.J.R. Hughes, "Finite Element Method for Piezoelectric Vibration", *Int. J. Num. Meth. Eng.*, Vol. 2, pp. 151 - 157 (1970)
5. Y. Kagawa and T. Yamabuchi, "Finite Element Simulation of Two-Dimensional Electromechanical Resonators", *IEEE Son. Ultrason.*, Vol SU-21 (4) pp. 275 - 283 (1970)
6. D.F. Ostergaard and T.P. Pawlak, "Three-dimensional finite elements for analyzing piezoelectric structures", *Proc. 1986 IEEE Ultrason. Symp.*, pp. 639 - 642 (1986)
7. R. Lerch and H. Kaarmann, "Three-Dimensional Finite Element Analysis of Piezoelectric Media", *Proc. 1987 IEEE Ultrason. Symp.*, pp. 853 - 858 (1987)
8. G.L. Wojcik, D.K. Vaughan, N. Abboud, J. Mould, "Electromechanical Modeling using Explicit Time-Domain Finite Elements", *1993 IEEE Ultrason. Symp.*, pp. 1107 - 1112 (1993)
9. B. Fornberg, *A Practical Guide to Pseudospectral Methods*, Cambridge University Press, (1996) ISBN 0-521-49582-2
10. J.-P. Berenger, "A perfectly matched layer for the absorption of electromagnetic waves," *J. Comp. Phys.*, Vol. 114, pp. 185 - 200 (1994)
11. G. Wojcik, B. Fornberg, R. Waag, L. Carcione, J. Mould, L. Nikodym, T. Driscoll, "Pseudospectral Methods for Large-Scale Bioacoustic Models", *Proc. 1997 IEEE Ultrason. Symp.* pp. 1501 - 1506 (1997)
12. T. Furumura, B. L. N. Kennett, and H. Takenaka "Parallel 3-D pseudospectral simulation of seismic wave propagation" *Geophysics* 63, 279, 1998